ELSEVIER

Ceramics International 30 (2004) 1383–1387

CERAMICS INTERNATIONAL

www.elsevier.com/locate/ceramint

Observations on structural evolution and dielectric properties of oxygen-deficient pyrochlores

Huiling Du [a,b,*], Hong Wang [a], Xi Yao [a]

[a] *Electronic Materials Research Laboratory, Key Laboratory of the Ministry of Education, Xi'an Jiaotong University, Xi'an 710049, China*
[b] *Department of Materials Science and Engineering, Xi'an University of Science and Technology, Xi'an 710054, China*

Received 28 November 2003; received in revised form 8 December 2003; accepted 22 December 2003

Available online 6 May 2004

Abstract

Non-stoichiometric ceramics with the series oxygen-deficient pyrochlore in Bi_2O_3–ZnO–Nb_2O_5 ternary system was investigated to obtain structural information. Crystal structure and dielectric properties of the group of $Bi_{1.5-2x}Zn_{1+2x}Nb_{1.5}O_{7-x}$ (with $x = 0$–0.3) compositions have been studied. The compounds departured badly from stoichiomeric compositions lead to structural distortion and unbalance of pyrochlore phase, till secondary phase occurs for $x = 0.3$. It can be inferred from Raman spectra that the concentration and ratio of species occupied B site is stable, while those of species occupied A site vary between the series compositions. It is reasonable to reckon that zinc dominantly occupies B site in pyrochlore structure with compositions varying. The experimental results show that dielectric constant (ε) decrease linearly while the temperature coefficient of dielectric constant (α_ε) effectively increases with increasing of the *x*-value. Crystal distortion and structural defect resulting from chemical composition unbalance bring on the change of dielectric properties for the small *x*-value.
© 2004 Published by Elsevier Ltd and Techna Group S.r.l.

Keywords: A. Powders: solid state reaction; B. Defects; C. Dielectric properties

1. Introduction

Among the ternary oxides, compounds of the general formula $A_2B_2O_7$ (A and B are metals) represent a family of phases with pyrochlore structure. Depending on the composition, those compounds exhibit a wide variety of interesting physical properties and applications: dielectric, piezo- and ferro-electric behavior, ferrimagnetism, giant magnetoresistance, semiconducting behavior or either metallic or ionic conduction. Oxides with the pyrochlore structure, $A_2B_2O_7$, furnish a host lattice suitable for incorporation of alivalent dopants, interstitial oxygen, protons, and electronic defects. The properties can possible be tailored within wide limits by doping on the A and B site. In any case, the physical properties are believed to be sensitive to the presence of oxygen vacancies and the observed of an anomalous lattice parameters dose not provide any information about the precise metal geometry or the oxygen non-stoichiometry [1,2].

It is well known that the structure of pyrochlore is a derivative of the fluorite structure where the unit cell is doubled and A site is divided into both A and B sites. The pyrochlore structure, of general stoichiometry $A_2B_2O_6O'$, can be described as two interpenetrating networks. The smaller B cations are octahedrally coordinated to O-type oxygens, the BO_6 octahedra sharing corners to give a B_2O_6 sublattice, which can be considered as the back-bone of the structure. The cage-like holes of this network contain a second sublattice A_2O', not essential for the stability of the structure: both A and O′ atoms may be partially or totally absent, as happens in certain families of defect pyrochlores AB_2O_6 [3]. Most defect pyrochlores have oxygen vacancies on the O′ site, although some are also non-stoichiometric with respect to the A-type cations. Departure from stoichiometry sometimes results in more complex derivative structures of pyrochlore [4]. A few $A_2^{1+}B_2^{5+}O_6$ phases are known (for example, $Tl_2Nb_2O_6$) in which an oxygen ion is absent; vacancies may also occur in the cation arrangement in $A^{1+}B^{5+}B^{6+}O_6$ compounds, for which K(NbW)O_6 provides an illustration. Some oxygen-deficient pyrochlores such as $Pb_2Ru_2O_{6.5}$ exhibit a long-distance ordering of the oxygen vacancies [5–7].

The accurate structural information now available for a number of binary non-stoichiometric pyrochlore oxides

* Corresponding author. Fax: +86-29-82668794.
E-mail address: hldu@xust.edu.cn (H. Du).

0272-8842/$30.00 © 2004 Published by Elsevier Ltd and Techna Group S.r.l.
doi:10.1016/j.ceramint.2003.12.091

with the type $A_{2-y}B_2O_{7-z}$. If y and z are both less than 0.5, then the oxides tend to adopt a regular pyrochlore structure, where the oxygen vacancies are randomly distributed on the O′ sites [8]. However, the focus of the present study on non-stoichiometric oxides is mainly limited in ion-conducting pyrochlores [9–12], the non-stoichiometric Bi-based dielectrics have not been investigated in details. Bismuth pyrochlore structured dielectrics have received much attention for device applications due to their high dielectric constant, low dielectric dissipation, and relatively low firing temperature [13–15].

The present paper outlines the results of a more detailed study on dielectric properties of new defective pyrochlores with the general formula $Bi_{1.5-2x}Zn_{1+2x}Nb_{1.5}O_{7-x}$ ($0 \leq x \leq 0.3$), along with detailed characterization of the structural changes associated with oxygen-deficient. The aims of the current paper are two-fold. Firstly, to describe the structural trend in non-stoichiometric pyrochlore oxides with particular emphasis on the variation in the lattice parameter and the cation distribution at A and B sites verses the x-values. And secondly, to examine the relationship between site occupation and dielectric properties.

2. Experimental

Samples were prepared by conventional solid-state methods. Raw materials (Bi_2O_3, ZnO, and Nb_2O_5) were weighed according to the composition $Bi_{1.5-2x}Zn_{1+2x}Nb_{1.5}O_{7-x}$, where $x = 0$, 0.05, 0.1, 0.2, and 0.3, respectively. The weighed batches were wet milled in planetary type for 4 h containing distilled water and agate balls. After drying, they were calcained at 800 °C for 2 h. Discs with 12 mm in diameter and 1 mm in thickness were prepared by uniaxial pressing. Finally, the pellets were sintered at temperatures up to 1100 °C in air. X-ray diffraction (XRD) patterns of the sintered ceramics were obtained at room temperature, by using a rotatory anode Rigaku Dmax-2400 X-ray diffractometer (Cu Kα radiation). Lattice parameters were refined by a least square refinement procedures. Raman spectra were recorded on selected polished pellets at room temperature with a Nicolet 950 FT-Raman Spectrometer with a spectral resolution of 2 cm^{-1}. The detector was a InGaAs detector and the excitation source was a Nd:YAG laser with an excitation wavelength of 1064 nm at 7500 mW. Low-fire silver electrodes were used for dielectric measurements. The dielectric constant and dissipation factor of samples were measured using a high precision LCR meter (HP 4284A). Resistivity data were obtained using a HP 4339A high-resistance meter at a measuring voltage of 100 V. The temperature dependence of the dielectric constant was measured at four different frequencies (10,100 K and 1 MHz) and temperature varying from RT to 500 °C by placing the discs in an automated measurement system consisting of a PC computer, a HP 4284A LCR meter and a temperature chamber.

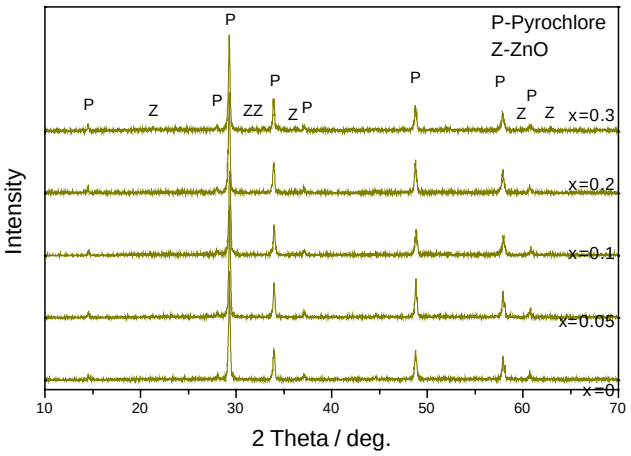

Fig. 1. XRD patterns of non-stoichiometric pyrochlores.

3. Results and discussions

Fig. 1 displays X-ray diffraction patterns of as-sintered samples of stoichiometric pyrochlore and non-stoichiometric pyrochlore. Bi-based oxides with the composition $Bi_{1.5-2x}Zn_{1+2x}Nb_{1.5}O_{7-x}$ where $x = 0$ adopt an ideal cubic pyrochlore-type structure with the oxygen vacancies randomly distributed over the 8b sites. All diffraction peaks of samples with compositions $x \leq 0.2$ were indexed as those of cubic pyrochlore structure. In the composition $x = 0.3$, small peaks of cubic zinc oxides phase was detected (JCPDS 13-0311) due to the notable chemical composition unbalance. In the series of defective pyrochlores, a slightly decrease in lattice parameter was observed with increasing x. The decrease of the lattice constant is attributed to invoking of smaller size of zinc ion than bismuth ion.

The crystalline BZN based defect pyrochlores were also examined by Raman spectroscopy to look for short-range differences. Cubic pyrochlores, $A_2B_2O_6O'$, belong to the space group $Fd3m$, where $z = 8$. The corresponding factor group for the cubic pyrochlore is O_h. The site symmetry is D_{3d} for A and B ions, C_{2v} for the O ions and T_d for the O′ ion, which is in accordance with previous reports [16,17].

On the basis of the crystal structure of cubic pyrochlores and group theoretical analysis, the optical phonon modes of pyrochlore compounds at the Brillouin-zone center are classified into

$$\Gamma^{*2}_{\text{opt.}} = A_g^{(R)} + 3A_{2u}^{(i.a)} + E_g^{(R)} + 3E_u^{(i.a)} + 2F_{2g}^{(i.a)} + 7F_{1u}^{(IR)} + 4F_{2g}^{(R)} + 4F_{2u}^{(i.a)}$$

Further, out of these 25 normal codes, only A_g, E_g, $4F_{2g}$ are Raman active and $7F_u$ are infrared active. The rest, $2F_g$, $3A_{2u}$, $3E_u$, and $4F_{2u}$ are optically inactive. So there are six active modes in Raman spectra, A_{1g}, E_g, and $3F_{2g}$ are attributed to O-sublattice vibrations and F_{2g} is assigned to O′-sublattice vibration.

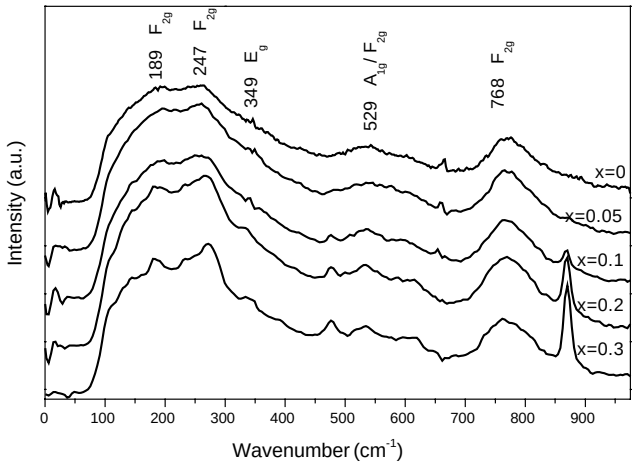

Fig. 2. FT-Raman spectra of the oxygen-deficient pyrochlore oxides.

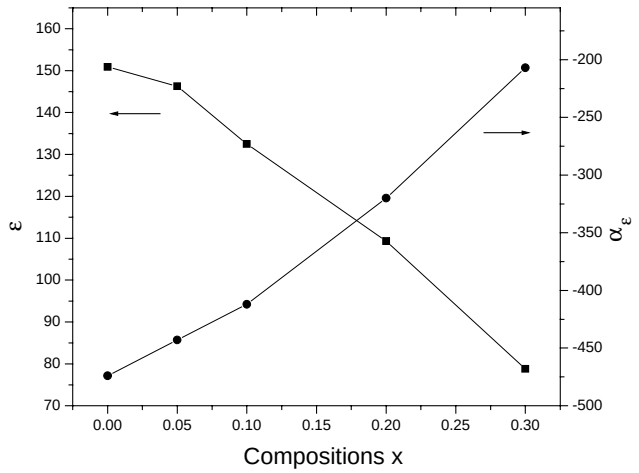

Fig. 3. The dielectric properties of defective pyrochlores dependence of compositions.

The Raman spectra from the stoichiometric BZN pyrochlores are dominated by three intense bands at 247, 529, and 768 cm^{-1} as shown in Fig. 2. For complex BZN based compounds, two species ions located at A and B site would lead to two different vibration bands. For example, the lowest frequency lines, 189 and 247 cm^{-1}, which are undoubtedly assigned to the F_{2g} mode. Table 1 gives the assignment of Raman shifts for all compounds. It is clear that when excess Zn^{2+} is invoked in the structure, slight shifts of the vibrational frequencies and the peak splitting are observed. The most notable difference for the various samples is the significant increase of Raman shifts at 247 cm^{-1} in intensity and full-width-at-half-maximum (FWHM) with x increasing. The Raman shift, intensity and FWHM of the Zn–O stretching mode of A site at approximately 247 cm^{-1} exhibited an increase in number of bonds duo to excessive of Zn ions introduction with x increasing. While the broad bands of the Nb–O band and Zn–O stretching mode at about 768 cm^{-1} exhibited hardly any variation between the various crystalline pyrochlore compositions, that indicate the concentration of Nb^{5+} and Zn^{2+} ions at B site keep stable but the ions concentration in A site varies with the chemical constitution change. Two new bands appear at 476 and 870 cm^{-1} as the x-value reaches 0.1, which shows single cubic pyrochlore from XRD results. Most probably results from a lowering of the space symmetry due to local disorder in the B-sublattice or from the existence of a significant amount of structural defects.

With x increasing, the Bi^{3+} concentration decreases and the Zn^{2+} concentration increases. The most probable ion distribution mechanism is corresponding adjusting of Bi^{3+} and Zn^{2+} at A site while keeping stable of concentration for Nb^{5+} and Zn^{2+} at B site, to yield oxygen non-stoichiometric pyrochlores, $(Bi_{1.5-2x}Zn_{0.5+2x})(Zn_{0.5}Nb_{1.5})O_{7-x}$, and so, structural defects such as oxygen vacancy and cations vacancy can form due to the valence compensation. It is reasonable to reckon that zinc ions is inclined to occupy B site firstly, and then enter into A site after the B site was fully occupy.

The dielectric properties of those defective pyrochlores are sensitive to the composition and sintering temperature. The composition dependence of dielectric properties at 1 MHz of series samples is shown in Fig. 3. It was found that the dielectric constant decreased with the increase in x-value. The dielectric constant for stoichiometric ceramics (where $x = 0$) is 150, and with increasing x decreases linearly down to 78 for high Zn content compositions (where $x = 0.3$). On the other hand, the temperature coefficient of dielectric constant (α_c) effectively increases from one end member ($\alpha_c = -474$ ppm/°C for $x = 0$) to the other end member ($\alpha_c = -207$ ppm/°C for $x = 0.3$). The tendencies

Table 1
Experiment peak position of Raman spectra and the types of the corresponding vibrational mode of oxygen-deficient BZN pyrochlores

Tentative assignment	Observed bands for oxygen-deficient pyrochlores (cm^{-1})				
	$x = 0$	$x = 0.05$	$x = 0.1$	$x = 0.2$	$x = 0.3$
"Breathing" of Bi cations	16	17	17	17	17
Bi–O stretching	189	189	185	182	182
Zn–O stretching	247	253	259	268	275
"Breathing" of O atoms	349	346	344	337	333
O–B–O bond bending	529	529	532	534	534
B–O stretching	768	768	768	765	765

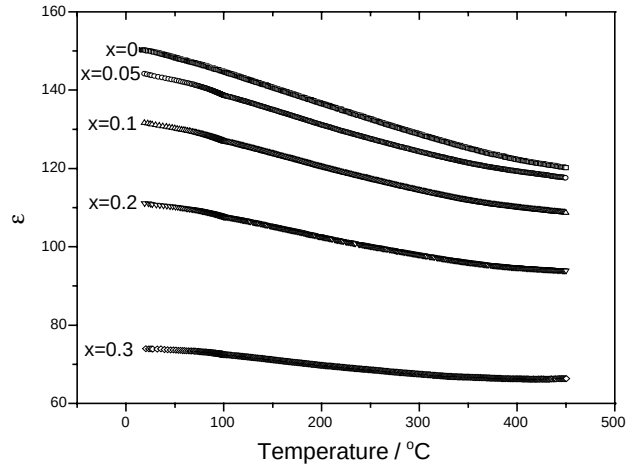

Fig. 4. Temperature dependence of the dielectric constant at 1 MHz for defective pyrochlores.

of the dielectric behavior versus temperature for all samples are similar, with the small negative temperature coefficients for samples with higher oxygen content deficiencies.

As oxygen-deficient ceramics have the more interesting characteristics as we anticipated, the temperature dependence of dielectric properties at various frequencies were studied. The temperature dependence of dielectric constant at 1 MHz of series samples is shown in Fig. 4. Fig. 5 shows the variation of the dielectric constant and dissipation factor of composition $x = 0.3$ with temperature, at several selected frequencies. It can be noticed the dielectric constant diminishes with the rise in the temperature region from RT to 300 °C and increases promptly above 350 °C. The dependence of dielectric loss on temperature is more sensitive. An intensely increased dielectric constant and loss is observed for all samples at temperatures above 350 °C. The higher the *x*-value, the lower the onset temperature. Such variations are strongly dependent on the frequencies, with losses at high frequencies much lower than those occurring at low frequencies. This kind of dependence of ε and tanδ on frequency is typically associated with losses by conduction [18]. On increasing the temperature, the electrical conductivity increases due to the increase in thermally activated drift mobility of electric charge carriers according to the hopping conduction mechanism. Therefore, the dielectric polarization increases causing a marked increase in ε and tanδ as the temperature increases.

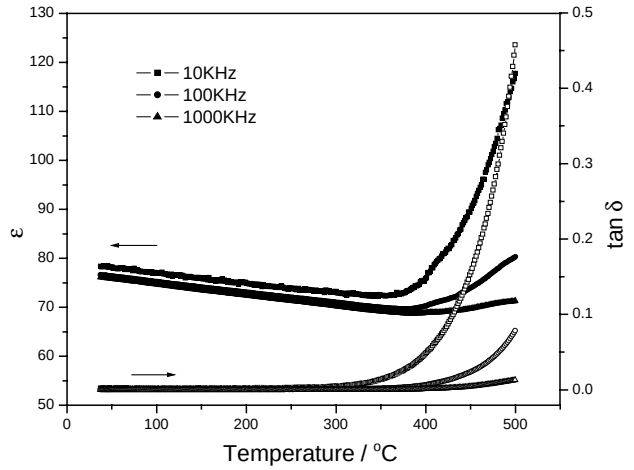

Fig. 5. The variation of the dielectric constant and dissipation factor of composition $x = 0.3$ with temperature, at various frequencies.

As we know, the dielectric constant of ceramics is based on the contribution to dielectric polarization from ions, electrons and defect structure within the materials. As for pyrochlore structure oxides, the dielectric constant is mainly derived from the ionic polarization and electronic polarization. Cations occupied different site have different ionic radius and polarizability. With the increase in *x*-value, the contribution of ions to dielectric constant change due to concentration and ratio of those ions inside ceramics varies, so dielectric constants for each composition are different. In the series pyrochlore structure compositions, the excess incorporation of Zn^{2+} with low polarizability will lead to the decrease in dielectric constant. For $x = 0.3$ compositions, where oxygen content in the structure is 30% lower, dielectric constant diminish to 78 due to unbalance of chemical compositions. So it is likely to consider that dielectric properties of non-stoichiometric BZN pyrochlores depend intensely on structural defects and phase evolution. Crystal distortion and structural defect resulting from chemical composition unbalance bring on the change of dielectric properties for the small *x*-value. Moreover, structural defects and second phase are responsible for the apparent deterioration of their dielectric properties for $x > 0.2$.

Here, we report the structure and dielectric characterization of new materials in the BZN based defective pyrochlore system in the vicinity of ambient temperature. This basic work will be useful for further investigation and understanding the crystal structure and physical properties of non-stoichiometric pyrochlores.

4. Conclusions

Series solid solutions of defective pyrochlores in the Bi_2O_3–ZnO–Nb_2O_5 system were prepared and investigated. XRD results indicate that samples for compositions $x \leq 0.2$ have a cubic structure with a gradual decrease of the lattice parameter with increasing *x*. The secondary phase occurs results from notable chemical composition unbalance when $x = 0.3$. Local structure is investigated by Raman spectra and shows that the concentration and ratio of species occupied B site is stable, while those of species occupied A site vary between the series compositions. It can be inferred that zinc ions is inclined to occupy B site firstly, and then enter into A site after the B site was fully occupy.

Dielectric properties vary remarkably with composition in oxygen-deficient pyrochlores. The experimental results show that dielectric constant decrease significantly while the

temperature coefficient shifts to small negative value with increasing of the *x*-value. Crystal distortion and structural defect resulting from chemical composition unbalance bring on the change of dielectric properties for the small *x*-value. Moreover, the existence of a significant amount of structural defects and second phase are responsible for the apparent deterioration of their dielectric properties for $x > 0.2$.

Acknowledgements

This work was supported by the Ministry of Science and Technology of China through 973-project under grant 2002CB613302.

References

[1] P.K. Moon, M.A. Spears, H.L. Tuller, in: B.C. Larson, M. Ruhle, D.N. Seidman (Eds.), Characterization of the Structure and Chemistry of Defects in Materials, 138 Materials Research Society Proceedings, Pittsburgh, 1989.
[2] P.J. Wilde, C.R.A. Catlow, Defects and diffusion in pyrochlore structured oxides, Solid State Ionics 112 (3–4) (1998) 173–183.
[3] F.J. Rotella, J.D. Jorgensen, B. Morosin, R.M. Biefeld, Deuterium sites in the defect pyrochlore DTaWO6: location from neutron power diffraction data, Solid State Ionics 5 (1981) 455–458.
[4] M.A. Subramanian, G. Aravamudan, G.V. Subba Rao, Oxide pyrochlores—a review, Prog. Solid State Chem. 15 (2) (1983) 55–143.
[5] Ismunandar, B.J. Kennedy, B.A. Hunter, Observations on pyrochlore oxide structures, Mater. Res. Bull., 34 (8) (1999) 1263–1274.
[6] R.E. Carbonio, J.A. Alonso, J.L. Mart′ýnez, Oxygen vacancy control in the defect $Bi_2Ru_2O_{7-y}$ pyrochlore: a way to tune the electronic bandwidth, J. Phys.: Condens. Matter 11 (2) (1999) 361–369.
[7] P. Garnier, J. Moreau, J.R. Gavari, Analyse de Rietveld de la structure de $Pb_{1-x}Ti_xO_{1+x}$ par diffraction des neutrons (Rietveld analysis of the structure of $Pb_{1-x}Ti_xO_{1+x}$ by neutron diffraction), Mater. Res. Bull. 25 (8) (1990) 979–986.
[8] F. Beech, W.M. Jordan, C.R.A. Catlow, A. Santoro, B.C.H. Steele, Neutron powder diffraction structure and electrical properties of the defect pyrochlores $Pb_{1.5}M_2O_{6.5}$ (M = Nb, Ta), J. Solid State Chem. 77 (2) (1988) 322–335.
[9] Y. Shimakawa, Y. Kubo, T. Manako, Giant magnetoresistance in $Tl_2Mn_2O_7$ with the pyrochlore structure, Nature 379 (6560) (1996) 53.
[10] J. Isasi, M.L. Lopez, M.L. Veiga, C. Pico, Ionic conductivity of a new defect pyrochlore, Solid State Ionics 89 (3–4) (1996) 321–326.
[11] B. Li, J. Zhang, Electrical conductivity of cadmium oxide–antimony oxide system ceramics, J. Am. Ceram. Soc. 72 (12) (1989) 2377–2380.
[12] M. Pirzada, R.W. Grimes, J.F. Maguire, Incorporation of divalent ions in $A_2B_2O_7$ pyrochlores, Solid State Ionics 161 (1–2) (2003) 81–91.
[13] M.F. Yan, H.C. Ling, W.W. Rhodes, Low-firing, temperature-stable dielectric compositions based on bismuth nickel zinc niobates, J. Am. Ceram. Soc. 73 (4) (1990) 1106–1109.
[14] D.P. Cann, C.A. Randall, T.R. Shrout, Investigation of the dielectric properties of bismuth pyrochlores, Solid State Commun. 100 (7) (1996) 529–534.
[15] H.L. Du, X. Yao, Evolution of structure and dielectric properties on bismuth-based pyrochlore with TiO_2 incorporation, J. Electroceram. 9 (2) (2002) 119–124.
[16] B.E. Scheetz, W.B. White, Characterization of anion disorder in zirconate $A_2B_2O_7$ compounds by Raman spectroscopy, J. Am. Ceram. Soc. 62 (9–10) (1979) 468–470.
[17] H.C. Gupta, S. Brown, N. Rani, V.B. Gohel, A lattice dynamical investigation of the Raman and the infrared frequencies of the cubic $A_2Hf_2O_7$ pyrochlores, J. Phys. Chem. Solids 63 (3) (2002) 535–538.
[18] M.A.L. Nobrea, S. Lanfredi, Impedance spectroscopy analysis of high-temperature phase transitions in sodium lithium niobate ceramics, J. Phys.: Condens. Matter 12 (35) (2000) 7833–7841.